# PARAMETRIC FINITE ELEMENT MODEL FOR
# SPIRAL WELDED PIPE SECTIONS LOADED IN TENSION

K. Van Minnebruggen[1], P. Thibaux[2], J. Van Wittenberghe[2], R. Denys[1], W. De Waele[1]

[1] Ghent University, Laboratory Soete, Belgium
[2] OCAS NV, ArcelorMittal Global R&D, Belgium

**Abstract:** Spiral welded pipes gain interest for oil and gas transportation in strain based design projects. Here, the structural response of the pipe with an environmentally imposed global plastic strain is of critical importance. However, a current lack of knowledge about the structural response of a spiral welded pipeline hinders the application in a strain based design context. This response is not only influenced by material properties, but also by geometrical characteristics. To understand these complex phenomena, finite element simulations can be considered. The finite element models need to incorporate all important factors to obtain a representative analysis. This paper describes the approach and structure used to develop such model. To obtain a high degree of automation and flexibility, the authors have developed a parametric script that allows creating a three dimensional curved wide plate test geometry taken from a spiral welded pipe.

The model allows to modify pipe geometry, weld and heat affected zone geometry and material properties including Hill's 1948 yield criterion to account for anisotropic material response. Pipe geometry includes helical forming angle, diameter, pipe profile and wall thickness with possible thickness variations. Weld and heat affected zone geometry include geometrical weld reinforcement of root and/or cap, fusion line profile and misalignment. A flaw, with variable size, is introduced in the weld metal or heat affected zone. To obtain an accurate description of the actual geometry, coordinate transformation schemes are incorporated that start from a flat plate with a simplified girth weld geometry. It is concluded that the proposed model is ready for use with a good view on mesh quality and output accuracy.

**Keywords:** Finite Element Modeling; Spiral Welded Pipe; Curved Wide Plate

## 1    INTRODUCTION

Since the demand for energy is ever growing, fossil fuels are nowadays extracted in increasingly hostile environments and remote locations. Pipelines that transport these hydrocarbons from source to user often traverse challenging regions, including discontinuous permafrost, landslides or ground settlements. These environmentally imposed loads can exert longitudinal deformations of the pipe beyond the elastic range of the steel used for the production of the pipeline [1,2]. To take these situations in account during the design stage, a strain based approach is used, which limits the allowable environmentally imposed strain in the pipe's axial direction rather than the occurring stresses.

Spiral welded pipes gain interest for use in strain based designed projects due to economical benefits in comparison with traditionally used UOE pipelines [3]. Recent developments in steel coil production have enabled the possibility to manufacture spiral welded pipes of high grade steel with sufficient wall thickness, strength and toughness properties [4,5,6]. However, no in depth research has been performed to assess their applicability in a strain based design context [7]. The ability to evaluate the structural response of a spiral welded pipeline subjected to an environmentally imposed plastic deformation is critical. To improve the understanding of these complex phenomena, finite element models can be used as an analysis tool.

A parametric three dimensional model has been developed, representing a curved wide plate (CWP) specimen taken in axial direction from a spiral welded pipe. This specimen, typically 300 mm wide, is commonly used to evaluate the strain capacity of (welded) pipes. Since it balances cost and amount of assessed material. This paper describes the approach and possibilities of the designed parametric numerical model. Attention is directed to geometry, material definition and numerical accuracy of the simulation results. The experimental validation and the relationship with full pipe behavior is part of future work and, therefore, beyond the scope of this paper.

## 2 FINITE ELEMENT MODEL

An in-house developed Python script generates FE models of CWP specimens containing spiral welds using the software package Abaqus® (version 6.11). It is based on a previously developed and successfully validated model for CWP specimens containing girth welds [8]. The original model is limited to one half of the specimen by making use of symmetry boundary conditions. The presented model analyses a full specimen rather than a half specimen, since the specimen is no longer symmetrical along its length direction. The new script has the possibility to alter the angular position of the weld region. A meshing scheme has been developed to achieve this without large mesh distortions.

### 2.1 Geometrical outline

#### 2.1.1 Overall dimensions

A curved wide plate specimen taken from a spiral welded pipe is schematically presented in Figure 1. The simulation should respect the original pipe geometry including the inner diameter ($D_i$ in mm), wall thickness ($t$ in mm) and the forming angle ($\alpha$ in °) of a spiral welded pipe. The forming angle can be varied up to 60 degrees, which is well beyond the range of 20 to 40 degrees that is most common for the production of high grade spiral pipes. Additional parameters characterizing the overall geometry are: the total length ($2L_{tot}$ in mm), the total specimen width ($2W_{tot}$ in mm), the length of the prismatic section ($2L$ in mm), the prismatic section width ($2W$ in mm), the shoulder cut-out radius ($R_s$ in mm), the notch length ($2c$ in mm) and the notch depth ($a$ in mm).
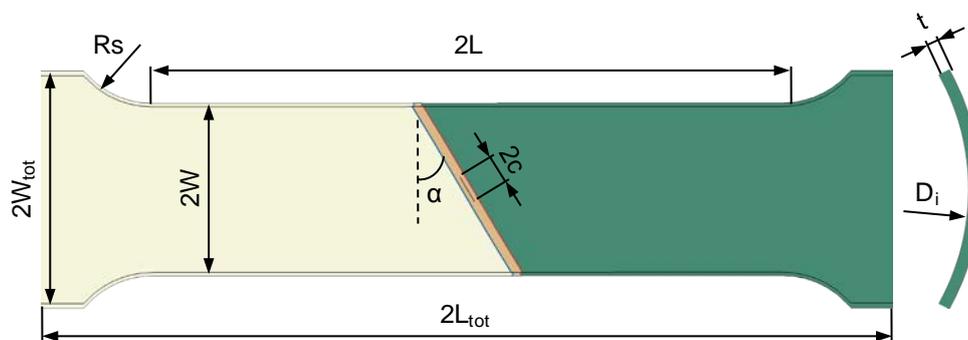


Figure 1: Spiral curved wide plate specimen.

The three dimensional numerical model starts from a rectangular flat plate with simplified shape. It consists of three dimensional linear elements with reduced integration and hourglass control (Abaqus® type C3D8R). The pipe curvature and helical weld are introduced using a sequential coordinate transformation of the finite element nodes [8]. Additionally, it is possible to introduce side skelp bending, which is typically applied during the production of spiral pipe. These transformations result in the finalized curved wide plate geometry with parameter controlled variable dimensions as indicated on Figure 1. To obtain an adequate mesh without excessive distortions, the notch length to prismatic section width ratio - $c/W$ - should be limited to 0.4.

#### 2.1.2 Weld and heat affected zone geometry

To represent actual spiral seam welds, the weld and heat affected zone (HAZ) should geometrically match. Therefore, a simplified rectangular weld geometry is transformed as illustrated in Figure 2. A basic geometry outline is used to introduce the elementary components of the weld region: the base materials which are connected by the weld, the weld material and the accompanying heat affected zones. Because the weld produced could show differences in mechanical properties at root and cap (filler), $h_{cap}$ (mm) is defined as the height of the cap material. Both heat affected zones are defined with a constant width.
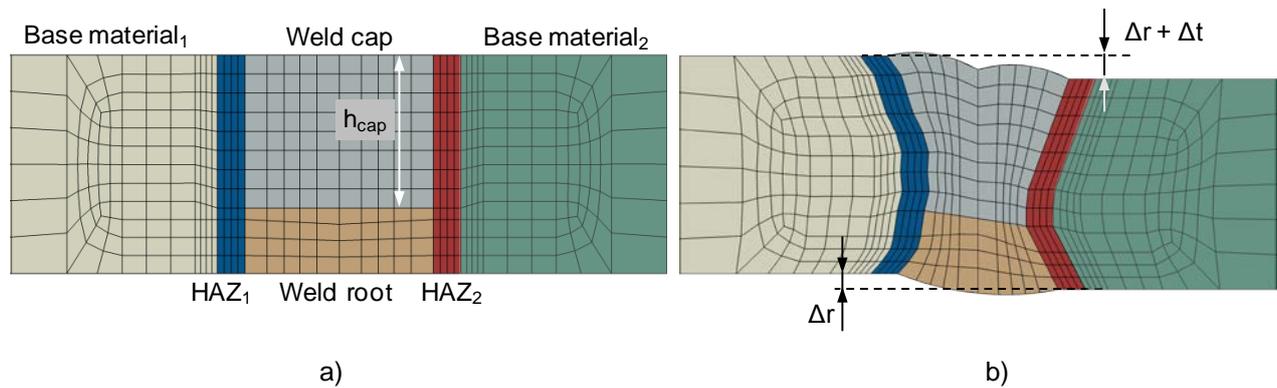
Figure 2: Weld and HAZ geometry: a) simplified rectangular sectioning, b) complex weld region geometry after coordinate transformation of mesh to represent actual experimental geometries

The final weld geometry can be simplified using a V-, X- or K-shaped outline. A more accurate representation can be made based on a point-wise weld geometry definition, as illustrated in the left HAZ region of Figure 2 b). Additional geometrical modeling options are: geometrical reinforcement of weld root and/or cap, a thickness variation ($\Delta t$ in mm) and/or a relative radial misalignment ($\Delta r$ in mm) of the skelp material between both sides of the weld. The geometrical reinforcement is modeled as a (single or multi) circular geometry as illustrated in Figures 2 b).

### 2.1.3   Artificial notch

An artificial notch is implemented in the numerical model to analyze the influence of inevitable weld flaws. The model is restricted to surface breaking flaws, i.e. embedded flaws cannot be analyzed. This is considered to be a conservative approach since surface flaws are more critical in terms of structural integrity. Concerning notch geometry, a semi-elliptical notch (Figure 3) or a notch with constant depth and semi-circular ends can be modeled.
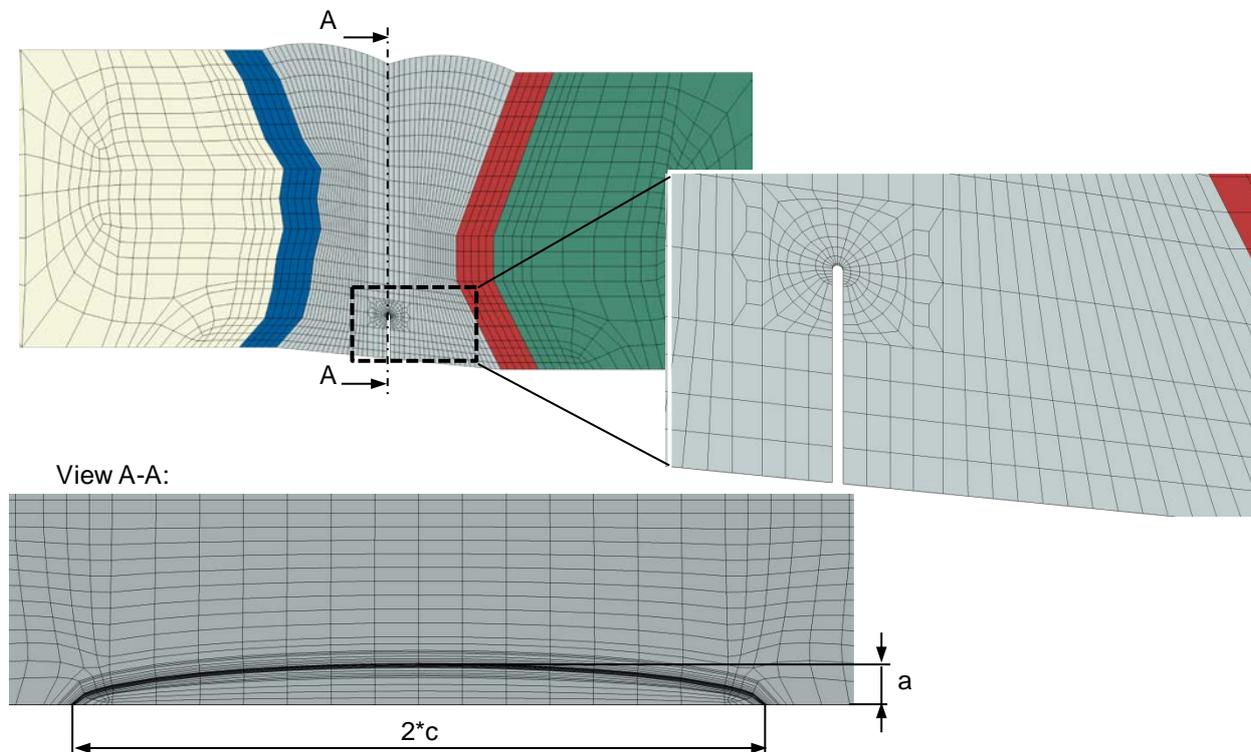


Figure 3: Semi-elliptical notch outline at weld metal centerline with spider web mesh.

Notch dimensions are parametrical; the notch depth ($a$ in mm), the notch length ($2c$ in mm) and the notch tip radius ($r$ in mm), which can be modeled as low as 2.5 µm. This is nearly equivalent to an infinitesimally sharp crack in numerical fracture mechanics analysis [9,10]. A single notch can be applied at the weld metal centerline or in the boundary of weld and HAZ material and at the inner or outer wall of the pipe.

An intelligent section partitioning and meshing scheme provides a consistent and structured mesh over the entire specimen, resulting in a coarse mesh at the specimen ends and a fine in the weld region. More particularly, in the vicinity of the notch, the mesh is refined to a spider web mesh (Figure 3) with element sizes close to one tenth of the notch radius. The mesh refinement has been numerically optimized as discussed in section 2.3.2.

## 2.2 Material properties

### 2.2.1 Base, weld and HAZ metal

The skelp mechanical properties can be heterogeneous along the length, which introduces a difference in stress-strain behavior at both sides of the helical weld for the spiral curved wide plate specimen. Therefore, specific material properties can be assigned to represent two different base metals. Consequently, also both HAZs can be assigned different stress-strain properties. For the weld metal, an additional sectioning is introduced to represent a possible difference between weld root and weld cap properties as discussed in section 2.1.2.

Each metal can be modeled as a point-wise stress-strain representation. Various simplified material responses can be chosen for each material individually, e.g.: the straightforward Ramberg-Osgood model and the more advanced UGent stress-strain model for line pipe steels [11,12].

### 2.2.2 Anisotropic material response

Skelp line pipe steel is traditionally produced using thermo-mechanical by controlled processing, which results in an anisotropic material response. To this extent the Hill's 1948 yield criterion, which is an extension of the Von Mises yield criterion, is implemented Eqs.(1) and (2).

$$\sigma_H = \left[ F\left(\sigma_{11} - \sigma_{22}\right)^2 + G\left(\sigma_{22} - \sigma_{33}\right)^2 + H\left(\sigma_{33} - \sigma_{11}\right)^2 + 2L\sigma_{23}^2 + 2M\sigma_{31}^2 + 2N\sigma_{12}^2 \right]^{1/2} \tag{1}$$

where the parameters $F$, $G$, $H$, $L$, $M$, $N$ are given by Eq. (2). In this equation $\sigma_{ij}$ is the measured yield stress value when $\sigma_{ij}$ is the only nonzero applied stress component. Next, $\sigma_0$ is the user-defined reference yield stress. The factors $R_{ij}$ represent the anisotropic yield stress ratios.

$$F = \frac{1}{2}\left(\frac{1}{R_{22}^2} + \frac{1}{R_{33}^2} - \frac{1}{R_{11}^2}\right); \quad G = \frac{1}{2}\left(\frac{1}{R_{33}^2} + \frac{1}{R_{11}^2} - \frac{1}{R_{22}^2}\right); \quad H = \frac{1}{2}\left(\frac{1}{R_{11}^2} + \frac{1}{R_{22}^2} - \frac{1}{R_{33}^2}\right);$$

$$L = \frac{3}{2R_{23}^2}; \quad M = \frac{3}{2R_{13}^2}; \quad N = \frac{3}{2R_{12}^2}; \quad \text{with}: R_{ii} = \frac{\sigma_{ii}}{\sigma_0}; R_{ij} = \frac{\sigma_{ij}}{\sigma_0/\sqrt{3}} \tag{2}$$

The Hill's yield criterion is a simplified anisotropic implementation which introduces a shift in the principal and combined directions (Figure 4).
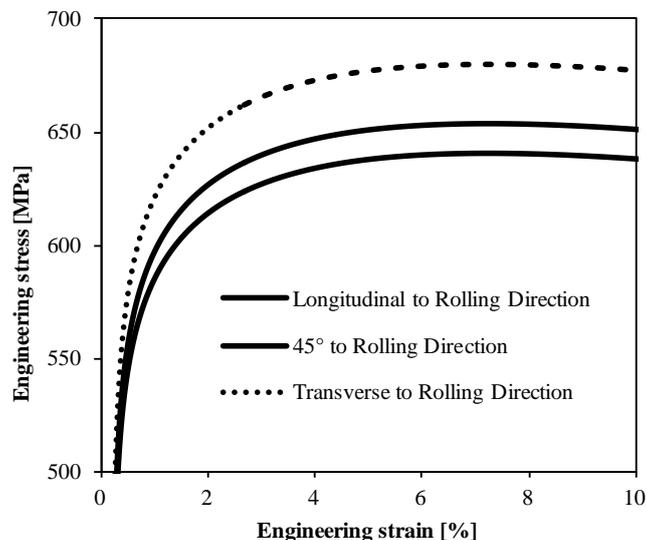


Figure 4: Base material strength in different directions defined as shift of longitudinal to rolling direction stress-strain behavior by +4% for the transverse strength and -2% for the 45 degrees strength.

## 2.3    Output and accuracy

### 2.3.1    Numerical output

In order to relate the numerical model to experimental data, several outputs are extracted during the post-processing of the model. Of particular relevance are: the crack mouth opening displacement (*CMOD*), the crack opening displacement in the vicinity of the notch tip (*COD*), the J-integral in the notched region, strain measurements by means of virtual LVDTs and strain gauges at various locations of the specimen surface in each direction (e.g. related to pipe global or skelp rolling directions).

The notch will be subjected to a mixed mode fracture behavior of mainly mode I and mode III as indicated on Figure 5. Therefore, CMOD and COD are measured perpendicular to the notch and in the pipe axial direction. The total value is calculated as the vectorial sum of the mode I and mode III components, see equation (3) [13].
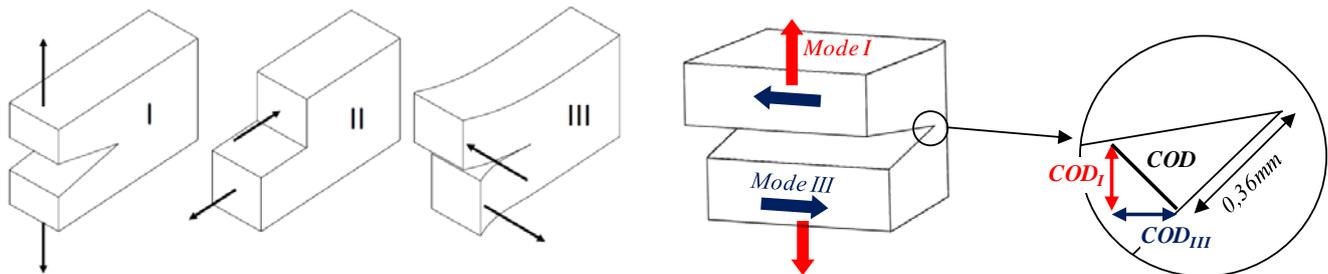


Figure 5: Three modes of fracture behavior: pure tensile (Mode I) and shear (Mode II and III).

$$CMOD = \sqrt{CMOD_I{}^2 + CMOD_{III}{}^2}$$

$$COD = \sqrt{COD_I{}^2 + COD_{III}{}^2}$$

(3)

To obtain an accurate result, the COD and CMOD are monitored by tracking two nodes. The COD nodes are positioned in accordance with [14] at a distance of 0.36 mm plus the original notch radius above the original notch tip. The CMOD can be monitored at the surface of the specimen at the notch flanks or at a discrete remote location to represent a clip gauge. To obtain an accurate J-integral evaluation a finer spider-web mesh is created in the vicinity of the notch tip, see Figure 3. Mesh size can be locally reduced in a parametric manner to facilitate analysis convergence without requiring an excessive increase of calculation time.

To evaluate strain capacity, the remote and overall strain in the base metal needs to be monitored. The LVDTs (LVDT$_{remote1}$ and LVDT$_{remote2}$) with a length *W* have to be located in regions of uniform strain field throughout the width of the specimen in order to eliminate boundary influences (Figure 6). To this purpose, their positions have been based on previous guidelines [15,16]. The overall strain can be monitored by LVDT$_{overall}$ spanning across the weld.
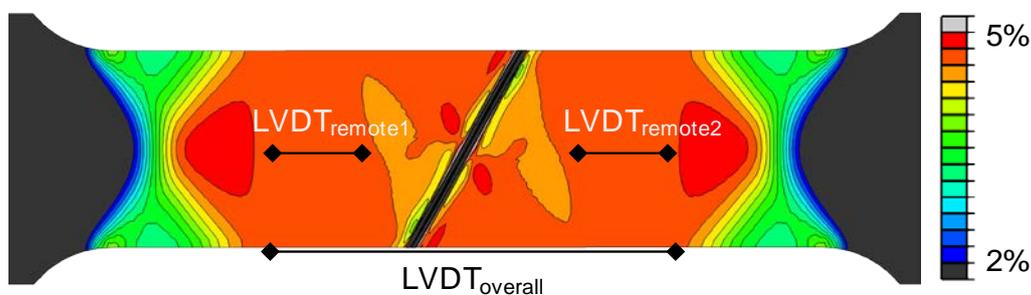


Figure 6: LVDTs are positioned in an area that is no longer influenced by the boundary conditions of the specimen ends.

Plastic strain hotspots develop near the shoulder regions of the specimen. To allow for an adequate measurement of the applied remote strain (i.e. in regions of uniform strain, away from the hotspots), the prismatic and total specimen length should be at least equal to:

$$2L = 3W(2 + \sin\alpha)$$
$$2L_{tot} = 4W(2 + \sin\alpha)$$

(4)

### 2.3.2   Accuracy

The mesh refinement topology allows for different mesh densities in various zones. This topology has been optimized to obtain a trade-off between accuracy and calculation time. A benchmark geometry (pipe diameter of 914 mm, wall thickness of 16 mm and a forming angle of 30 degrees) has been used and similar results were obtained for multiple geometry variations. A model with first order elements with as much as 300.000 nodes has been used as a reference case. Table 1 presents the error relative to the reference case of three coarser mesh topologies. The data has been obtained at maximum applied force, when necking initiates (i.e. force reduces with increasing plastic elongation). As such, the specimen is considered to fail due to plastic collapse.

Table 1. Mesh convergence study on desktop with four cores at 3 GHz.

|  | Reference | Case 1 | Case 2 | Case 3 |
|---|---|---|---|---|
| Number of Nodes | 300.000 | 125.000 | 65.000 | 35.000 |
| Smallest element size [μm] | 20 | 30 | 40 | 60 |
| Number of elements through thickness; weld – base metal | 18 - 12 | 14 - 8 | 10 - 6 | 5 - 3 |
| Total processing time [min] | 900 | 240 | 90 | 40 |
| Force error [%] | / | 0.0 | 0.0 | 0.1 |
| COD error [%] | / | 0.3 | 1.7 | 3.2 |
| CMOD error [%] | / | 0.4 | 1.5 | 3.5 |
| Remote Strain error [%] | / | 0.1 | 1.1 | 1.9 |

Based on Table 1 and considering a relative numerical error of less than 2% as required for all outputs, the mesh topology of case 2 will be used for future analysis.

## 3   CONCLUSIONS

A three dimensional model of a spirally welded curved wide plate specimen loaded in tension has been developed. Model creation, analysis and post-processing are fully parametric, and therefore highly suited for systematic studies involving a substantial amount of simulations. The obtained accuracy is a well-balanced trade-off between calculation time and numerical accuracy. The validity of the model will be experimentally evaluated by means of actual wide plate sections loaded in tension. This validation is essential to obtain trustworthy results based on the numerical model.

## 4   ACKNOWLEDGEMENTS

## 5   REFERENCES

[1]   Kan W. C., Weir, M., Zhang, M. M., Lillig, D. B., Barbas, S. T., Macia, M. L., and Biery, N. E., (2008). "Strain-Based Design: Design Consideration Overview," Proc 18th International offshore and Polar Engineering Conference, ISOPE, Vancouver, BC, Canada, pp 174-181.

[2]   Lillig D. B., (2008). "The First Isope Strain-Based Design Symposium - A Review," Proc 18th International offshore and Polar Engineering Conference, ISOPE, Vancouver, BC, Canada, pp 1-12

[3]   Bian Y., Penniston C., Collins L., and Mackenzie R., (2008) "Evaluation of UOE and Spiral-Welded Line Pipe for Strain Based Design," Proc 8th International Pipeline Conference, Calgery, Canada.

[4]   Liebeherr M., Güngör Ö.E., Quidort D., Lèbre D., and Ilic N., (2011) "Development and Weldability Assessment of Heavy Gauge X80 Linepipe Steel for Spiral Welded Pipe", CBMM Welding of High Strength Pipeline Steels international Seminar, Araxa, Brazil, November.

[5]   Yuqun, Y., Yixin, H., Yongkuan, Y., Daoyuan, W., Yonglong, W., and Stalheim, D. G., (2008) "The Development of X80 Steel Plate and Coil for The 2nd West-East Pipeline Project," Proc 7th International Pipeline Conference, Calgary, Alberta, Canada.

[6]   Güngör Ö.E., (2010) "Welding Evaluation of 21.6 Mm X80 Linepipe Steel From Coil", The 2nd South East European IIW international Congress, Sofia, Bulgaria.

[7]   Van Minnebruggen, K., De Waele, W., Denys, R., and Thibaux, P., (2012), "Strain based design considerations for spiral welded pipelines", Proc of 4th Sustainable Construction and Design Conference, Ghent, Belgium.

[8]   Hertelé, S., De Waele, W., Denys, R., Verstraete, M., and Van Wittenberghe, J. (2012) "Parametric finite element model for large scale tension tests on flawed pipeline girth welds", Advances in Engineering Software 47, pp 24-34.

[9]   Cravero, S. and C. Ruggieri, (2003) "A two-parameter framework to describe the effect of constraint loss on cleavage fracture and implications for failure assessments of cracked components". Journal of Brazilian Society of Mechanical Sciences and Engineering, 15, pp 403 - 412.

[10] Ranestad, O., Z.L. Zhang, and C. Thaulow, (1999) "Quantification of geometry and material mismatch constraint in steel weldments with fusion line cracks". International Journal of Fracture, 99, pp 211-237.

[11] Hertelé, S., De Waele, W., Denys, R., (2011) "A generic stress–strain model for metallic materials with two-stage strain hardening behaviour", International Journal of Non-Linear Mechanics, 46(2011), pp 519 – 531.

[12] Hertelé, S., De Waele, W., Denys, R., and Verstraete, M., (2012) "Full-range stress-strain behaviour of contemporary pipeline steels: Part I. Model description", International Journal of Pressure Vessels and Piping, 92, pp 34 - 40

[13] Liu, M., Wang, Y.-Y., and Collins, L., (2012), "Tensile strain capacity of spiral pipes", Proc 9th International Pipeline Conference, IPC, Calgary , Alberta, Canada.

[14] Fairchild, D.P., Macia, M.L., Kibey, S., Wang, X., Krisham, V.R., Bardi, F., Tang, H., and Cheng, W., (2011) "A Multi-Tiered Procedure for Engineering Critical Assessment of Strain-Based Pipelines", Proc 21st International Offshore and Polar Engineering Conference, ISOPE, Maui, Hawaii, USA, pp 698 – 705.

[15] Denys, R.M., and Lefevre, A., (2009) "UGent guidelines for curved wide plate testing", Pipeline Technology Conference, Ostend

[16] Hertelé, S., De Waele, W., Denys, R., and Verstraete, M., (2012) "Investigation of strain measurements in (curved) wide plate specimens using digital image correlation and finite element analysis", Jounal of Strain Analysis, 47 (5), pp 276 – 288.